12

Time Reversal Technique for Ultra Wide-band and MIMO Communication Systems

Ijaz Naqvi[1] and Ghaïs El Zein[2]
[1]*LUMS School of Science and Engineering (SSE) Sector U, D.H.A. Lahore Cantt*
[2]*European University of Brittany (UEB)*
INSA, IETR, UMR 6164, F-35708, 20 avenue des Buttes de Coesmes, 35708 Rennes
[1]*Pakistan*
[2]*France*

1. Introduction

Ultra wide band (UWB) technology gained a renewed interest after February 2002, when the Federal Communications Commission (FCC) approved the First Report and Order (R&O) for commercial use of UWB technology under strict power emission limits for various devices. The permission to transmit signals in a wide unlicensed band, opened the doors for the coexistence of UWB technology along with other narrow band and spread spectrum technologies. In UWB communication, extremely narrow RF pulses are employed to communicate between transmitters and receivers. Because of its extremely wide bandwidth, UWB signals result in a large number of resolvable multi-paths and thus reduce the interference caused by the super position of unresolved multi-paths. However, it also results in a complex receiver system. To collect the received signal energy, several kinds of receivers can be applied such as transmit-reference, Rake or decision feedback autocorrelation receiver. The later two techniques are quite complex while the former decreases the data rate of the system. One way to overcome these drawbacks is to make use of a technique that shifts the design complexity from the receiver to the transmitter.

Time Reversal (TR) has been proposed as a technique to shift the design complexity from the receiver to the transmitter. Classically, TR has been applied to acoustics Fink (1992); Fink & et. al. (2000) and underwater systems Edelmann et al. (2002), but recently, it has been widely studied for broadband and UWB communication systems Khaleghi et al. (2007)- Oestges et al. (2004). The received signal in a TR system is considerably focused in spatial and temporal domains and can be received using simple energy threshold detectors. The temporal and spatial focusing of the TR scheme improves with the bandwidth of the signal, therefore, systems with ultra wide bandwidth are inherently suitable for the TR scheme. One of the very first experimental study for TR with wideband electromagnetic waves is carried out in Lerosey et al. (2006). In a TR UWB communication systems, a time-reversed channel impulse response (CIR) is employed as a transmitter pre-filter. The TR technique comprises of two steps. In the first step, the CIR is estimated at the transmitter end. In the second step, the complex conjugated and time-reversed CIR is transmitted in the same channel. The TR wave then propagates in an invariant channel following the same paths in the reverse order. Finally

at the receiver, all the paths add up coherently in the delay and spatial domains. Experimental demonstration of TR UWB has been performed in Khaleghi et al. (2007); Naqvi & El Zein (2008). The performance of MISO TR systems has been analyzed in Kyritsi, Papanicolaou, Eggers & Oprea (2004); Qiu et al. (2006). TR performance in a multi-user scenario is studied in a number of articles Naqvi et al. (2007); Nguyen et al. (2006). The performance of TR UWB for different bandwidths is analyzed in Khaleghi & El Zein (2007). For dense multi-path propagation channels, strong temporal compression and high spatial focusing can be achieved with a focusing gain of about 8 dB Khaleghi et al. (2007). For communication purposes, this gain improves the transmission range. Inter symbol interference (ISI) effects are mitigated by temporal compression and multi-user interference is reduced due to spatial focusing. The received signal in a TR system is considerably focused in spatial and temporal domains and can be detected (or demodulated) using simple energy threshold detectors.
For the TR scheme, multiple-input single-output (MISO) TR has been used in the literature to exploit the diversity gain offered by the MISO configuration. In Kyritsi, Eggers & Oprea (2004); Kyritsi, Papanicolaou, Eggers & Oprea (2004), using the data from a fixed wireless 8×1 MISO measurement, a delay compression by a factor of 3 was shown to be possible. In Qiu et al. (2006), using the experimental results, temporal focusing and an increase in collected energy with the number of antennas in MISO-TR systems is verified.
In this chapter, we present results of TR validation with multiple antenna configurations using time domain instruments followed by the parametric analysis of the TR scheme. Different TR properties such as normalized peak power (NPP), focusing gain (FG), signal to side-lobe ratio (SSR), increased average power (IAP) and RMS delay spread are compared for different muli-antenna configurations. In the second part of the chapter, a modified transmission scheme for a multi user time-reversal system is proposed. With the help of mathematical derivations, it is shown that the interference in the modified TR scheme is reduced compared to simple TR scheme. Limitations of the proposed scheme are studied and an expression for maximum number of simultaneous users is proposed.

2. Introduction of Time Reversal

Time reversal (TR) is a transmission scheme in which time-reversed channel impulse response (CIR) is used as a transmitter pre-filter. In a first step, the CIR is estimated between a transmitter and a receiver. Then the CIR is flipped in time and emitted by the transmitter. The time-reversed wave back propagates in the channel following the same paths as the CIR's ones but in the reverse order. Finally at the receiver, all the paths add up coherently in the time and spatial domains. For dense multipath propagation channels, strong temporal compression and high spatial focusing can be achieved. High temporal compression reduces inter symbol interference (ISI) whereas spatial focusing reduces multi-user interference and ensures communication security. The noiseless received signal ($y_j(t)$) at the intended receiver (j) can be mathematically represented as:

$$y_j(t) = s(t) \star h_{ij}(-t) \star h_{ij}(t) = s(t) \star R_{ij}^{auto}(t) \tag{1}$$

where $h_{ij}(t)$ is the CIR from the transmitting point (i) to an intended receiver (j), $s(t)$ is the transmitted signal, $\star$ denotes convolution product and $R_{ij}^{auto}(t)$ is the autocorrelation of the

CIR, $h_{ij}(t)$. The noiseless received signal at any non intended receiver (k) is written as:

$$\begin{aligned} y_k(t) &= s(t) \star h_{ij}(-t) \star h_{ik}(t) \\ &= s(t) \star R_{ikj}^{cross}(t) \end{aligned} \tag{2}$$

where $h_{ik}(t)$ is the CIR from the transmitting point (i) to an unintended receiver (k) and $R_{ikj}^{cross}(t)$ is the cross-correlation of the CIR $h_{ik}(t)$ and $h_{ij}(t)$. If the channels are uncorrelated, then the signal transmitted for one receiver will act as a noise for a receiver at any other location. Thus, a secure communication is achieved with low probability of detection and low probability of interception.

In the practical implementation of the TR systems, the pre-coding filter is truncated in time to reduce the filter length and thus the system complexity. The truncated response is represented as $h'(-t)$. For data communication purpose, the transmitted symbols are modulated by a binary pulse amplitude modulation (BPAM) scheme. The k^{th} symbol, d_k, of the symbol sequence is equal to 1 or -1 for the data bits 1 or 0 respectively. Therefore, the received signal at the intended receiver is written as:

$$\begin{aligned} y(t) &= \underbrace{A \sum_k d_k h'(-t - k\,T_s)}_{\text{Transmitted RF signal}} \star \underbrace{h(t)}_{\text{CIR}} + n(t) \\ &\approx A \sum_k d_k R'_{hh}(t - k\,T_s) + n(t) \end{aligned} \tag{3}$$

where A is a normalization factor, T_s is the inter-symbol interval, $n(t)$ is the noise and $R'_{hh}(t)$ is the correlation between the truncated CIR ($h'(t)$) and the original CIR ($h(t)$). For the sake of simplicity we have supposed that the T_s is equal to the length of the measured time-reversed CIR ($h'(-t)$). As the amplitude of the peak of the received signal is proportional to the energy of the transmitted signal ($\int h'^2 dt$), the truncation process decreases the peak of the received signal. Due to BPAM, the polarity of the received signal peaks depends on the transmitted data bit and is used for the detection of the data bits.

3. Time-Reversal with multi-antenna configurations

The temporal compression and spatial focusing properties of the TR scheme makes it an attractive transmission scheme for MIMO systems. One of the main differences between a classical MIMO system and a MIMO-TR system is that in the classic system, the receiving antennas receive multiple superposed signals while in the TR system, each antenna receives only one dominant signal. The spatial focusing property of the TR means that the antennas which are separated in space will have uncorrelated channel impulse responses. Thus, the interference caused by the transmitted signals for unintended receiving antennas is suppressed. At the same time, the time dispersive characteristics of the channel are mitigated by the temporal compression inherent to the TR scheme. Therefore, simultaneous communication with all receiving antennas can be performed using simple detectors at the receiver Nguyen et al. (2006). The received signal with MIMO-TR for N_t transmitting antennas and N_r receiving antennas is given by the expression:

$$y_j(t) = \underbrace{s_j(t) \star \sum_{i=1}^{N_t} R_{ij}^{auto}(t)}_{Signal(j)} + \underbrace{\sum_{i=1}^{N_t} \sum_{k=1;k\neq j}^{N_r} s_k(t) \star R_{ikj}^{cross}(t)}_{Interference(j)} + \underbrace{n_j(t)}_{Noise(j)} \quad (4)$$

where $s_j(t)$ and $s_k(t)$ are the transmitted signals intended for the j_{th} and the k_{th} receiving antenna respectively and $n_j(t)$ is the added noise. There are two types of MIMO communications; one is the multiuser scenario and second is the single user MIMO scenario. In the first case, multiple transmitting antennas communicate with multiple receiving antennas well separated in space. In multi user TR communication, the interference part in (4) may be suppressed because of the large distances between the receiving antennas.

In a single user MIMO scenario, it might be possible to simultaneously transmit signals over several independent channels. (4) is valid in this case as well. Note that the number of users then becomes the number of the receiving antennas. Since the interference power increases with the number of receiving antennas, one cannot send more information by simply adding more receiving antennas. However, with reasonably smaller number of receiving antennas than the number of transmitting antennas and a rich multi-path environment, the desired signal's magnitude might become larger than that of the interference Nguyen et al. (2005). In this case, the application of TR in wireless MIMO could be possible.

MISO-TR has been investigated in a number of papers to benefit from the antenna diversity of the configuration. In Kyritsi, Eggers & Oprea (2004); Kyritsi, Papanicolaou, Eggers & Oprea (2004), using the data from a fixed wireless 8×1 MISO measurement, a delay compression by a factor of 3 was shown to be possible. In Qiu et al. (2006), using the experimental results, temporal focusing and an increase in collected energy with the number of antennas in MISO-TR systems is verified. Also, the reciprocity of realistic channels is demonstrated with the help of MISO-TR. MISO-TR system is investigated for UWB communication over ISI channels in Mo et al. (2007). TR is studied for a multi user scenario in Naqvi et al. (2007); Nguyen et al. (2005; 2006).

The use of multiple element antenna (MEA) systems in wireless communications has recently become a well-known technique to increase the transmission reliability and channel capacity Nguyen et al. (2005). Antenna and diversity gain can be achieved using available combining methods (selection, equal gain, maximum ratio combining). However, for wide-band MEA systems where signals are mixed both in time and space, a combination of advanced signal processing algorithms is required to overcome the effects of multi-path fading and ISI. Therefore, the receiver is expected to have a rather high complexity. Since the setup of MEA systems has some similarity to TR, it becomes an interesting question whether TR can be applied in MEA wireless systems. If this is the case, the advantages will be three fold: i) reducing ISI without the use of an equalizer ii) focusing the signal on the point of interest thereby reducing the interference and iii) applying a rather simple receiver structure.

In this chapter, validation of TR scheme is carried out with different multi-antenna configurations in the reverberation chamber (RC) and the indoor environment. A single user approach is applied for all configurations. Different multi-antenna configurations include SISO, SIMO (1×2), MISO (2×1) and MIMO (2×2). Time reversal (TR) measurements are conducted for ultra wide-band (UWB) signals in a RC for these multi-antenna configurations. A comparison is made among the four configurations. Channel measurement is done by using an arbitrary waveform generator (AWG) at the transmitter and a high speed digital

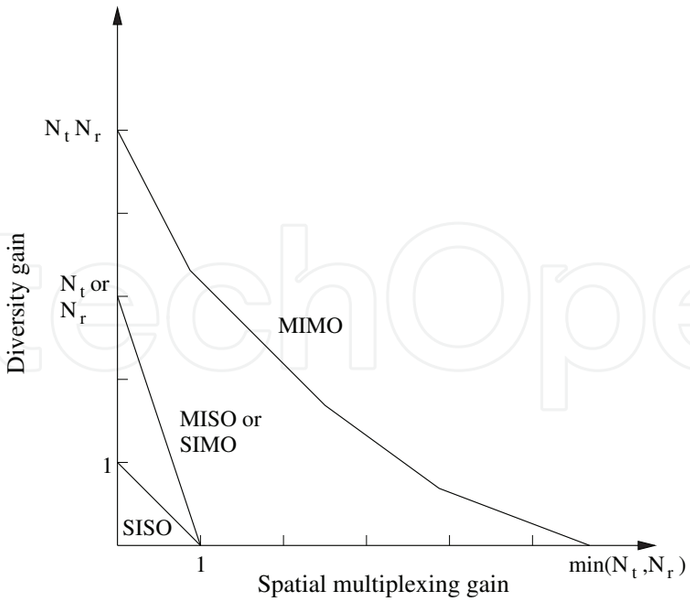

Fig. 1. Multiplexing and diversity gains for different multi antenna configurations

storage oscilloscope (DSO) at the receiver. For all these configurations, the received signals are time-reversed and re-transmitted from the transmitting antenna. TR performance is analyzed and compared for all the configurations by considering different TR characteristics i.e. normalized peak power (NPP), focusing gain (FG), signal to side-lobe ratio (SSR), increased average power (IAP) and RMS delay spread.

There are two types of gains associated with the configurations having more than one antenna either at the transmitting end or at the receiving end or both. One gain is the diversity gain achieved through the antenna diversity. The upper bound for the diversity gain is the product, $N_t N_r$, where N_t and N_r are the number of transmitting and receiving antennas respectively. The upper bound for the multiplexing gain is $min(N_t, N_r)$ Guguen & El Zein (2004). FIG. 1 further elaborates the limits of spatial multiplexing gain and the diversity gain for different multi antenna configurations.

In a TR system, same bounds for the multiplexing gain and diversity gain apply. We have compared different TR properties for different cases of MIMO configurations. The diversity gain is taken into account and the received signal in the case of SIMO and MIMO configurations is combined (or added) whereas transmitted signal is combined for MISO configuration. The results for the MIMO TR validation are published in Naqvi & El Zein (2009; 2010).

3.1 MIMO-TR in a Reverberation Chamber

A comparison of TR with different multi antenna configurations is first made in the RC. These experiments show performance of the TR scheme in an ideal static environment. Multi-antenna TR in the RC makes full use of the multi-path diversity inherent to the environment. The performance evaluation in an ideal environment only gives a general trend of the TR performance, therefore in order to validate our results, experiments are also conducted realistic indoor environment.

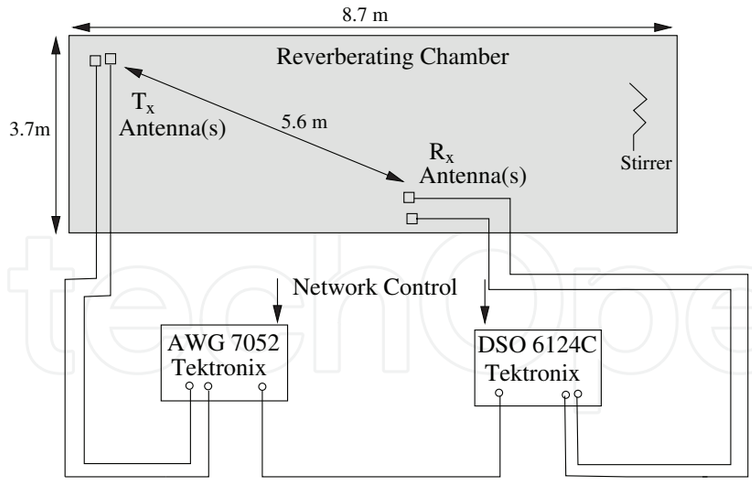

Fig. 2. Experimental setup for different multi-antenna configurations in the reverberation chamber

Fig. 3. The interior of the reverberation chamber with two conical monopole antennas

3.1.1 Experimental setup

An experimental setup is established in the RC for the validation of the TR in multi-antenna configurations. Measurement setup is illustrated in FIG. 2. A set of four conical mono-pole antennas (CMA) are used at the transmitter and receiver with both co-polar and cross-polar antenna orientations and different multi-antenna configurations. FIG. 3 shows two CMAs placed inside the RC. The height of the transmitter and the receiver is 1 *m* from the ground. The distance between the transmitter and receiver is 5.6 *m*. The channel sounding pulse with a rise time of 200 *ps* (see FIG. 4) and the time-reversed measured channel response (MCR) are generated through the AWG. The received signal is measured by a DSO. The DSO captures the MCR of the channel as well as the time-reversed response (TRR). The DSO is operated in average mode so that 256 samples are taken and averaged together to reduce the impact of noise.

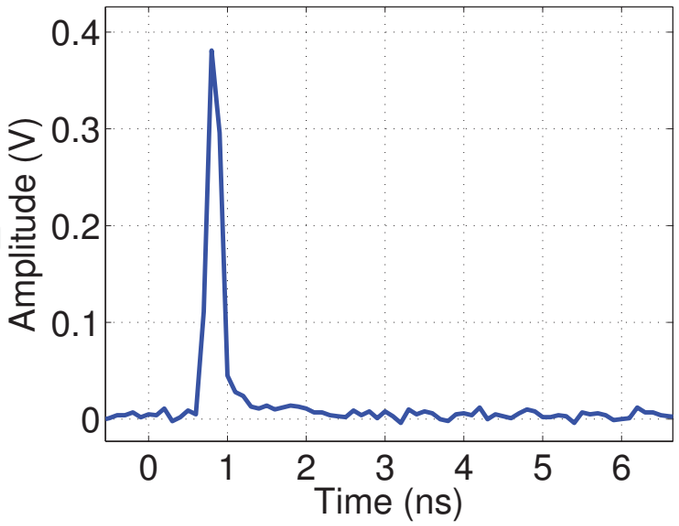

Fig. 4. Channel sounding pulse

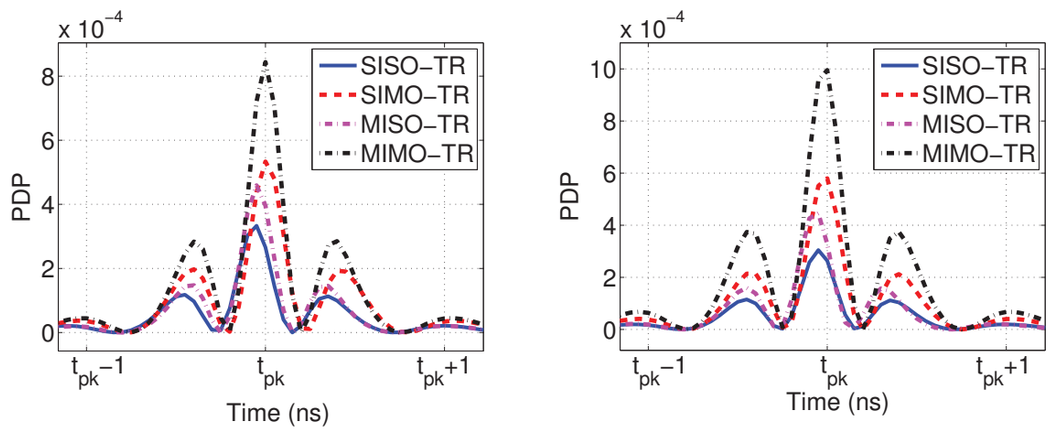

(a) Co-polar antenna orientation (b) Cross-polar antenna orientation

Fig. 5. PDP of the received TR signal with SISO, SIMO and MIMO configurations

3.1.2 Experimental results

FIG. 5 shows power delay profile (PDP) of the received TR signal in RC for SISO, SIMO, MISO and MIMO configurations for a fixed transmitted power with both co-polar and cross-polar antenna orientations. It is evident that MIMO, MISO and SIMO TR have a better TR peak performance compared to SISO-TR. The comparison for all TR characteristics for these configurations is summarized in Table 1. The peak power of the received signal is normalized to the SISO-TR received peak power. The normalized peak power (NPP) improves with SIMO, MISO and MIMO configurations. MIMO-TR outperforms SISO, SIMO and MISO TR for the same transmitted power. For instance, NPP MIMO-TR is 4.02 dB and 5.16 dB and more than the obtained values with SISO-TR for co-polar and cross-polar antenna orientations respectively.

TR Property	Co-polar antenna orientation				Cross-polar antenna orientation			
	SISO	SIMO	MISO	MIMO	SISO	SIMO	MISO	MIMO
$\sigma_\tau^{MCR}(\mu s)$	2.21	2.11	2.19	2.08	2.21	2.11	2.17	2.21
NPP (dB)	0	2.01	1.37	4.02	0	2.79	1.667	5.16
FG (dB)	26.05	24.62	27.32	27.41	28.02	27.47	30.46	30.67
SSR (dB)	4.51	4.29	4.93	4.68	4.22	4.32	4.43	4.24
IAP (dB)	3.59	4.09	5.02	5.94	3.40	4.50	5.20	5.89
$\sigma_\tau^{TR}(n s)$	0.54	0.57	0.50	0.50	0.52	0.54	0.48	0.55

Table 1. Time-reversal characteristics in the reverberation chamber with different polarizations and multi-antenna configurations

As for the other TR properties, the performance of all the configurations remains almost the same. The configurations which have multiple antennas at the transmitter (MISO and MIMO) have a better FG and IAP than the configurations having one antenna at the transmitter (SISO and SIMO). The SSR remains almost constant for all configurations. The RMS delay spread also remains constant for all configurations. As SSR and RMS delay spread affect the ISI, therefore, all the configurations have a similar signal to interference (SIR) performance. However, the bit rate of the system can be increased taking advantage from the multiplexing gain of multi-antenna configurations.

3.2 SISO and SIMO-TR in the indoor Environment

Experiments are carried out in the indoor environment for SISO and SIMO configurations for a cross-polar antenna orientation for both LOS and NLOS environments. The experimental setup is very similar to the experimental setup in the reverberation chamber except that the environment is different and a power amplifier is used for the measurement of channel response (see Fig. 6).

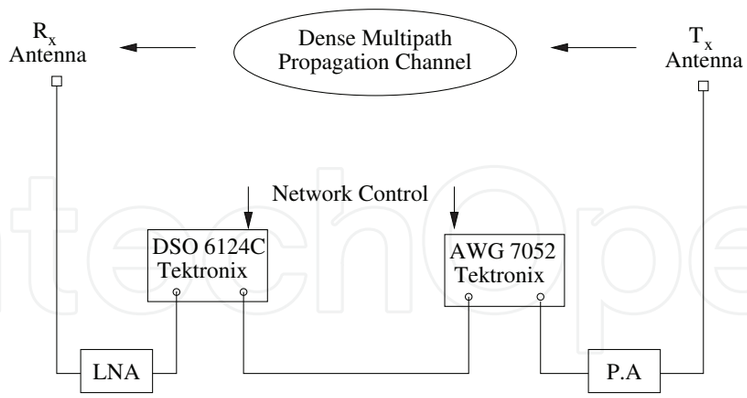

Fig. 6. Experimental setup

3.2.1 Experimental results

Fig. 7 shows for both LOS and NLOS configurations, the power delay profile (PDP) of the received TR signal in an indoor environment with SISO and SIMO configurations for a fixed transmitted power. It is obvious that SIMO TR has a better TR peak performance compared to SISO-TR. TABLE 2 compares different TR properties with SISO-TR and SIMO-TR in the indoor

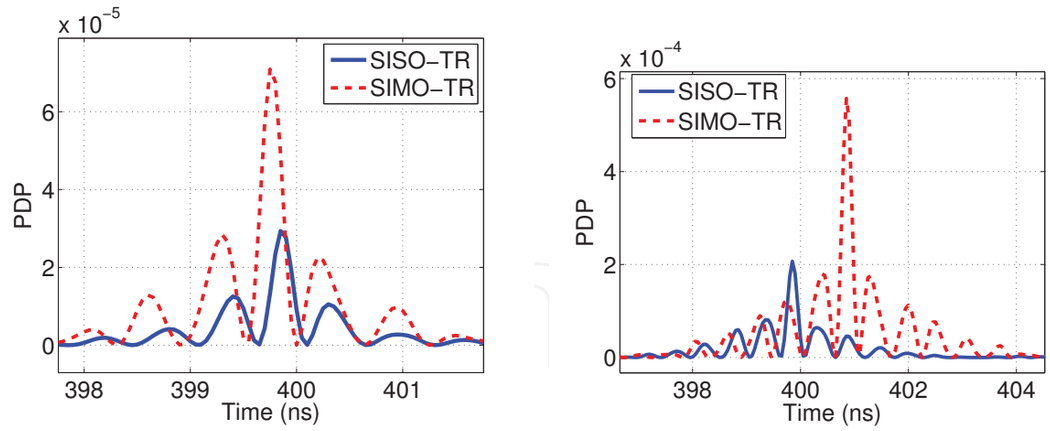

(a) LOS configuration (b) NLOS configuration

Fig. 7. PDP of the received TR signal with SISO and SIMO configurations in an indoor environment

TR Property	LOS		NLOS	
	SISO-TR	SIMO-TR	SISO-TR	SIMO-TR
NPP (dB)	0	4.30	0	3.81
FG (dB)	10.17	9.65	12.67	13.16
SSR (dB)	4.05	4.90	3.7	3.98
IAP (dB)	5.79	5.16	4.14	4.98
$\sigma_\tau^{TR}(ns)$	11.7	14.46	13.29	13.16
$\sigma_\tau^{MCR}(ns)$	18.35	16.07	23.21	22.17

Table 2. Time Reversal characteristics in the indoor environment with different SISO and SIMO configurations

environment. The NPP with SIMO-TR is 4.30 dB and 3.81 dB greater than the obtained values with SISO-TR in LOS and NLOS environments respectively. All other TR properties are very similar for SISO and SIMO-TR. NLOS environment has larger values for RMS delay spread of the MCR (σ_τ^{MCR}) but the RMS delay spread for the TR signal (σ_τ^{TR}) is in the same range for both LOS and NLOS environments.

4. Multi-user TR communications

In this part of the chapter, time-reversal (TR) communication is investigated by modifying the transmission prefilter. Mathematical expressions for received signal and the interference in the modified transmission scheme are derived. It is shown that the modified transmission approach reduces multi-user interference which eventually translates into a better bit error rate (BER) performance than simple TR multiuser scheme. Channel impulse responses (CIR) of a typical indoor channel are measured. In a multi-user scenario, both TR and the modified TR schemes are studied using the measured CIRs. It is shown that the proposed modified TR scheme outperforms the original TR scheme.

4.1 Description of the proposed transmission approach

In a multi user TR system, multiple signals for different users are transmitted simultaneously. The measured and truncated CIR from the transmitter to the user i can be written as:

$$h_i'(-t) = \sum_{m=0}^{L-1} a_m \delta(t - m\,\tau_s) \tag{5}$$

where L is number of time-reversal filter taps which corresponds to $T_{sig} = L\,\tau_s$ in time(seconds), a_m is the associated amplitude and $m\,\tau_s$ is the associated delay of the multi-path components. τ_s is the time between two consecutive samples and depends on the sampling rate of the time-reversal filter. For instance, if the measured CIR is sampled with a sampling rate of $5\,GS/s$, the delay of $\tau_s = 0.2\,ns$ is obtained. Therefore the number of taps (L) in filter having a length of $50\,ns$ is $L = 250$ samples or taps. The transmitted signal for multi user TR can be written as:

$$T_x(t) = \sum_{k} \sum_{i=0}^{N_u-1} \frac{1}{\sqrt{N_u}} d_{ik} A_i h_i'(-t - kT_s) \tag{6}$$

where d_{ik} is the k_{th} information bit of the i_{th} user, N_u is the total number of simultaneous users, T_s is the inter symbol interval and A_i is the normalization factor which can be written as:

$$A_i = \frac{1}{\sqrt{\left\| h_i'(-t - kT_s) \right\|^2}} \tag{7}$$

where $\|.\|$ is the Frobenius norm operation. The term $\frac{1}{N_u}$ insures that the signals for all the users are transmitted with a constant power. This is in contrast to Nguyen et al. (2006), where this normalization has not been carried out resulting in an unfair comparison of the performance with different number of users. Neglecting the noise, the received signal for the j_{th} user and the k_{th} symbol can be written as:

$$R_{x_{kj}}(t) = \underbrace{\frac{1}{\sqrt{N_u}} d_{jk}\, h_j(t) \star h_j'(-t + jT_u - kT_s)}_{Signal} + \underbrace{\frac{1}{\sqrt{N_u}} \sum_{i=0, i\neq j}^{N_u-1} d_{ik}\, h_j(t) \star h_i'(-t + iT_u - kT_s)}_{Interference} \tag{8}$$

The responses of the modified filter are produced by shifting $h'(-t)$ to either left or right and then forcing the shifted part to zero so that the shifted signal can be packed in the same signal duration. Fig. 8 shows the pattern of the left or right shift for $l = 1, 2$ taps. As shown for the left shift of 1 tap, the last three taps are shifted to left by one tap and the slot for last tap is filled with zero. For the right shift of 1 tap, first three taps are shifted to right and then the slot for the first tap is filled with zero. With the process of filling the shifted taps with zeros, we get rid of the unwanted signal, which causes interference to the adjacent symbols (called *Image* in Naqvi et al. (2009)). As the taps which result in an undesired signal are forced to

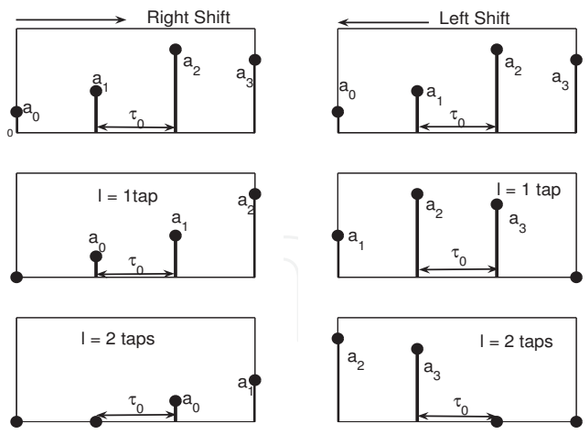

Fig. 8. Pattern for the left and right shift

zero, the received peak signal increases for an equal transmitted power. If $h'(-t)$ is shifted left by $T_u = l\,\tau_s$, the expression is given by:

$$\begin{aligned} left\,shift(h'(-t), T_u) &= \hat{h}(-t + T_u) \\ &= [\sum_{i=0}^{L-l-1} a_{i+l}\delta(t - i\,\tau_s)\,zeros(1, l)] \end{aligned} \tag{9}$$

where $zeros(1, l)$ is a vector containing l number of zeros, l is the number of taps required to carry out a shift of T_u seconds. Note that $\hat{h}(-t + T_u)$ has $L - l$ non zero taps. The transmitted signal with the modified transmission scheme can be thus written as:

$$T_x(t) = \sum_k \sum_{i=0}^{N_u-1} \frac{1}{\sqrt{N_u}} d_{ik}\,A_i \hat{h_i}(-t + iT_u - kT_s) \tag{10}$$

where $A_i = \frac{1}{\sqrt{\|\hat{h}(-t+iT_u-kT_s)\|^2}}$ and the term $\frac{1}{\sqrt{N_u}}$ insures that the power transmitted for different number of users is constant. The received signal for the k_{th} symbol of the j_{th} user can be written as:

$$\begin{aligned} R_{x_{kj}}(t) = & \underbrace{\frac{1}{\sqrt{N_u}} d_{jk} h_j(t) \star \hat{h_j}(-t + jT_u - kT_s)}_{Signal} \\ & + \underbrace{\frac{1}{\sqrt{N_u}} \sum_{i=0, i\neq j}^{N_u-1} d_{ik} h_j(t) \star \hat{h_i}(-t + iT_u - kT_s)}_{Interference} \end{aligned} \tag{11}$$

4.2 Interference analysis of the proposed scheme

To analyze the worst case performance, it is assumed that the transmitter communicates with all users at the same time. Therefore, TR received signal in a multi user scenario consists of a sum of one autocorrelation function and $N_u - 1$ cross correlation functions. The $N_u - 1$ cross correlation functions cause multi user interference. The received signal peak is the sum of the square of the coefficients of CIR (from the properties of the auto-correlation function). The interference term at the time of the peak (t_{peak}) for the j_{th} user in a simple TR scheme can be written as:

$$I_{j_{simple\,TR}}(t_{peak}) = \sum_{i=1, i\neq j}^{N_u} \sum_{m=0}^{L-1} b_{mi} \times a_{mj} \tag{12}$$

where b_{mi} are the coefficients of the time-reversed CIR $h'_i(-t + i\,T_u - k\,T_s)$ (from (8)) specific to the user i, a_{mj} are the coefficients of $h_j(t)$. As (12) uses simple TR transmission scheme, the high powered taps of $h'_i(-t)$ and $h'_j(-t)$ are approximately in the same time interval. Therefore, taps in the propagating channel containing more energy are multiplied by the taps of the transmitted signal with more energy resulting in a relatively higher interference.

To calculate the interference of the modified transmission scheme, we assume that the transmitted signal for the intended receiver is not shifted. Then by using (11) and (12), interference at the peak of the intended signal is then written as:

$$I_{j_{mod.TR}}(t_{peak}) = \sum_{i=0, i\neq j}^{N_u-1} \sum_{m=0}^{L-l-1} b_{(m+l)\,i} \times a_{mj} \tag{13}$$

where b_{mi} and a_{mj} are the same coefficients used in (12). Here the interference is the product of $L - l$ coefficients (as l taps are forced to zero). Furthermore, (13) suggests that in case of modified TR scheme, the taps in the propagating channel containing more energy are multiplied by the taps of the transmitted signal with less energy and vice versa. Therefore, interference is reduced with the new proposed transmission scheme. This reduced interference helps to improve the bit error rate (BER) performance of the system.

4.3 Effects of shift on received signal peak

In a TR communication system, as the received signal is the auto correlation function of the CIR, the received signal peak is the sum of the square of the coefficients of CIR. Neglecting the interference and the noise, the received signal peak with the modified TR scheme for the k_{th} symbol of the j_{th} user is written as:

$$R_{x_{modTR}}(t_{peak_{jk}}) = d_{jk}\, A_j \Big(\sum_{m=0}^{L-l_j-1} a_m^2 \Big) \tag{14}$$

where a_i are the coefficients of taps of $\hat{h}(-t + j\,T_b - kT_s)$ and l_j ($j\,\frac{T_b}{\tau_s}$) are the number of taps required for a shift of $j\,T_b$. The received signal peak depends on the energy contents of $(L - l_j)$ filter coefficients. Thus, the amplitude of the received peak decreases by the sum of the square coefficients in the shifted part of the transmitted signal. Therefore with the new modulation scheme, the received signal peak reduces in proportion to the energy of the shifted part of the transmitted signal.

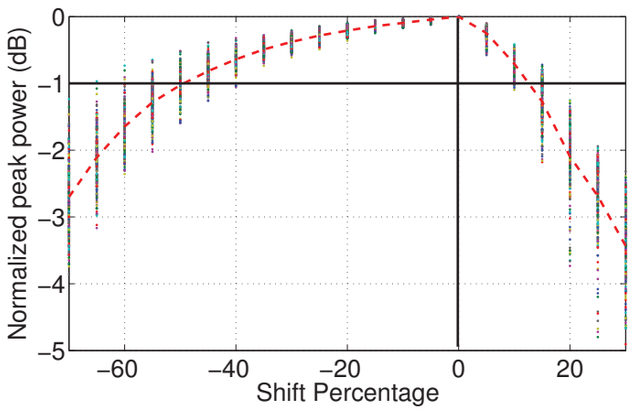

Fig. 9. Received signal peak power with left and right shifts normalized to the peak with no shift

Fig. 9 shows the peak power of the received signal peak for the shifted signals normalized to the received peak with no shift. The shift percentage corresponds to the percentage of the total length of the transmitted signal. A set of 243 measured CIRs are used for the simulation. Experimental setup and the measurement procedure are explained in Section 4.4. The loss of the received peak power for transmitted signals corresponding to individual CIRs is represented by the dots and the dashed line is the mean of power loss. To calculate the maximum number of simultaneous users that a system can support, we must take the decision in accordance to the threshold (say 3 dB) which can vary for different applications. For a 3 dB threshold, our system can support a shift percentage of $0.70L$ taps for left shift and $0.25L$ taps for right shift (see Fig. 9). Thus, the number of users with the proposed scheme can be written as:

$$N_u^{mod.TR} = \lfloor \frac{0.95 \times L}{\delta} \rfloor = \lfloor \frac{0.95 \times T_{sig}}{\Delta TR} \rfloor \tag{15}$$

where $\lfloor . \rfloor$ denotes the floor operator, L is the total number of taps in the transmitted signal, δ is the shift percentage between two simultaneous users, T_{sig} is the channel length in s and ΔTR is shift separation between two users in s. For the same threshold, the previously proposed scheme in Nguyen et al. (2006) can only support a shift of $0.75L$ which is contrary to their claim of 100% shift (as power loss with circular shift operation was not considered by the authors). The power loss for left shift is lesser than the power loss for the right shift as the energy contained in the shifted parts of the right shift is greater than the energy contained in the shifted parts of the left shift. Although a combination of right and left shifts can be used for the communication, for the sake of simplicity we have only used a left shift. In the rest of the paper unless otherwise mentioned, a shift is meant to be a left shift.

The power spectral density (PSD) of the transmitted signal of a TR communication system takes into account the effects of the antennas and the propagation channel including the path loss. In contrast to the pulse signal, the spectrum of a TR signal has a descending shape with increasing the frequency because the higher frequency components experience a greater path loss as compared to the lower frequency components in the spectrum. Fig. 10 shows the PSD plots of the transmitted signal with simple TR and modified TR schemes where a left shift of $0.20N$ taps is carried out for both modified TR scheme. The plots of both schemes have a descending shape. Maximum spectral power is experienced at the same frequency. Therefore,

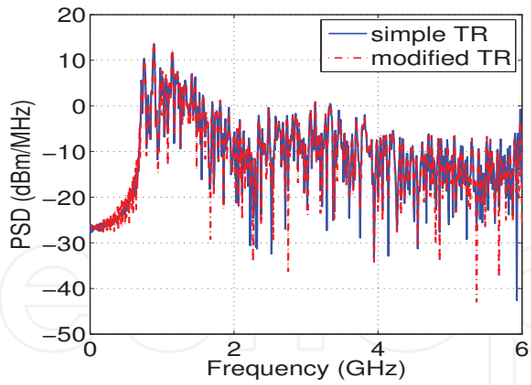

Fig. 10. PSD of transmitted signal with simple TR and modified TR schemes

both the signals must be attenuated with the same factor in order to respect the UWB spectral mask proposed by FCC. Frequency selectivity of the transmitted signals is similar for the two schemes. In short, the both schemes have resembling spectral properties.

4.4 Experimental setup and simulation results

Experiments are performed in a typical indoor environment. The environment is an office space of $14\,m \times 8\,m$ in the IETR[1] laboratory. The frequency response of the channel in the frequency range of 0.7-6 GHz is measured using vector network analyzer (VNA) with a frequency resolution of 3.3 MHz and two wide band conical mono-pole antennas (CMA) in non line of sight (NLOS) configuration. The height of the transmitter antenna and the receiver antenna is 1.5 m from the floor. The receiver antenna is moved over a rectangular surface ($65\,cm \times 40\,cm$) with a precise positioner system. The frequency responses between the transmitting antenna and receiving virtual array are measured. The time domain CIRs are computed using the inverse fast Fourier transform (IFFT) of the measured frequency responses.

4.5 BER performance

In the proposed transmission scheme, one user is separated with the other by a shift of a fixed number of taps. This separation is named as δ, which is a percentage of total number of taps in the transmitted signal. Signal for User 1 is transmitted without any shift. As discussed in Section 4.2, that interference between users is greatly reduced with the proposed modulation scheme. To study the impact of the reduced interference, we evaluate the BER performance with the proposed scheme using left shift for 5, 10 and 15 simultaneous user for $\delta = 0.05\,L$.
From the measured CIRs, we generate almost $35 \times (35 - N_u - 1)$ combinations for simulating different number of simultaneous users (N_u). For every combination of simultaneous users, 10000 symbols are transmitted which makes it sufficient for statistical analysis. The measured CIR is truncated for 90% energy contained in the CIR. Thus, the transmitted symbol has a length of $55\,ns$ and a per user bit rate of $18\,Mbps$. Perfect synchronization and no ISI effects are assumed. Signal to noise ratio (SNR) is varied by varying the noise variance, as:

$$SNR = P_j / \sigma^2_{noise} \tag{16}$$

[1] Institute of Electronics and Telecommunications of Rennes

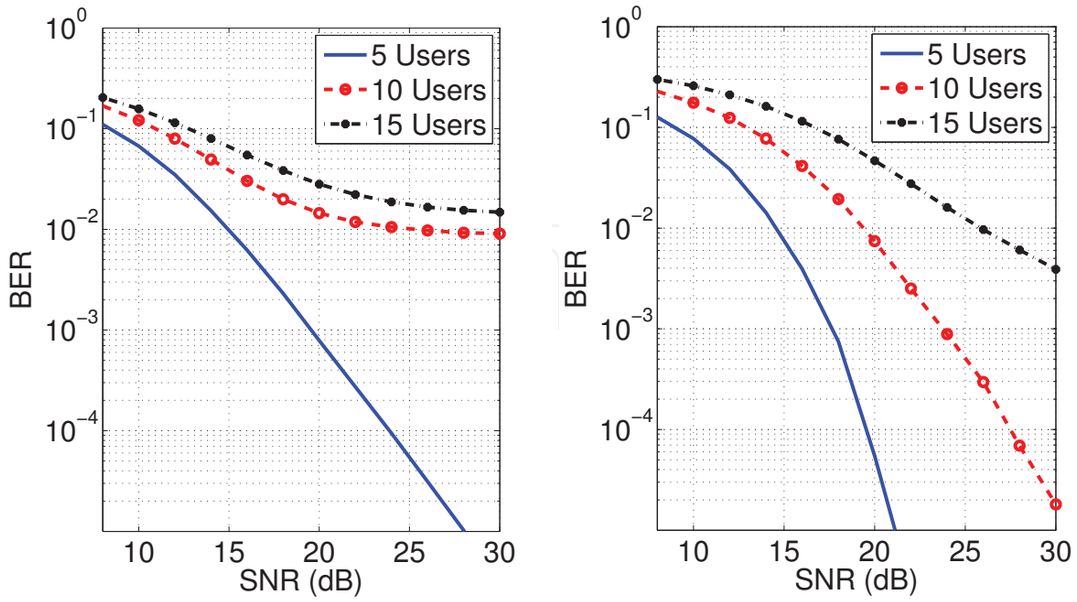

(a) Simple-TR

(b) TR with circular shift

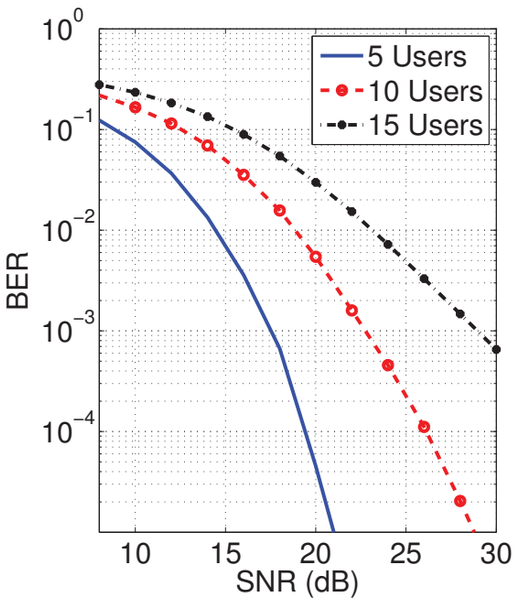

(c) Modified-TR scheme

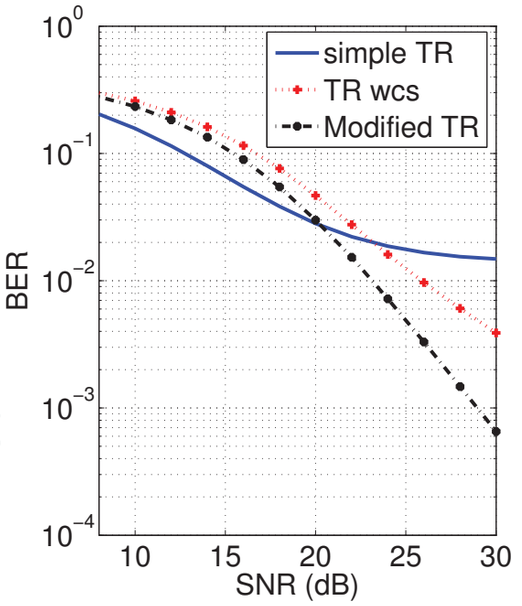

(d) All three schemes

Fig. 11. BER performance with 5, 10, and 20 simultaneous users with a) simple TR, b) TR with circular shift, c) modified TR scheme, d) 15 simultaneous users with all three schemes for $\delta = 0.05\,L$ taps

where P_j is the power of the received signal at its peak and σ^2_{noise} is the noise variance. Bipolar pulse amplitude modulation (BPAM) is used for these simulations. The received signal $y_j(t)$ is sampled at its peak and is detected based on ideal threshold detection, given as:

$$\text{Detected bit} = \begin{cases} 1 & \text{if } y_j(t_{peak}) \geq 0 \\ 0 & \text{if } y_j(t_{peak}) < 0 \end{cases} \tag{17}$$

Fig. 11a-c shows the BER performance of the simple TR, TR with circular shift operation and the modified TR scheme for 5, 10 and 15 simultaneous users. The modified TR scheme outperforms the other two schemes specially for higher number of simultaneous users (10, 15). For instance for 10 simultaneous users, the modified TR scheme results in a 1.4 dB better performance than the TR with circular shift for a BER of 10^{-4}. The simple TR scheme has already reached a plateau. To perform an analysis in the presence of extreme multi user interference, BER performance is studied for 15 simultaneous users. Fig. 11d compares the performance of the three schemes for 15 simultaneous users. The modified TR scheme gives significantly better performance than the other two schemes. The improvement is in the order of 4.5 dB or more.

If a system has a large number of users, the users experiencing higher shift percentages will give poorer performance than the users experiencing lower shift percentages. To have a consistent system, we propose to rotate the shift percentages for different users so that no user is subjected to permanent high shift percentage.

5. Conclusion

In this chapter, TR validation with multiple antenna configuration, followed by the parametric analysis of the TR scheme, is performed by using time domain instruments (AWG and DSO). Different TR properties such as normalized peak power (NPP), focusing gain (FG), signal to side-lobe ratio (SSR), increased average power (IAP) and RMS delay spread are compared for different muli-antenna configurations. It has been found that with multi-antenna configurations, a significantly better TR peak performance is achieved with all other properties remain comparable to the SISO-TR scheme.

In the second part of the chapter, a modified transmission scheme for a multi user time-reversal system is proposed. With the help of mathematical derivations, it is shown that the interference in the modified TR scheme is reduced compared to simple TR scheme. Limitations of the proposed scheme are studied and an expression for maximum number of simultaneous users is proposed. It is shown that the modified TR scheme outperforms simple TR and TR with circular shift scheme specially at higher number of simultaneous users. For instance for 15 simultaneous users, the modified TR scheme improves the performance in the order of 4.5 dB or more for a constant BER.

All these results suggest that the TR UWB, combined with MIMO techniques, is a promising and attractive transmission approach for future wireless local and personal area networks (WLAN & WPAN).

6. Acknowledgment

This work was partially supported by ANR Project MIRTEC and French Ministry of Research.This work is a part of ANR MIRTEC and IGCYC projects, financially supported by French Ministry of Research and UEB.

7. References

Akogun, A. E., Qiu, R. C. & Guo, N. (2005). Demonstrating time reversal in ultra-wideband communications using time domain measurements, *International Instrumentation Symposium*.

Edelmann, G., Akal, T., Hodgkiss, W., Kim, S., Kuperman, W. & Song, H. C. (2002). An initial demonstration of underwater acoustic communication using time reversal, *IEEE Journal of Oceanic Engineering* 27(3): 602–609.

Fink, M. (1992). Time reversal of ultrasonic fields-part i: Basic principles, *IEEE Transactions on Ultrasonics, Ferroelectrics and Frequency Control* 39(5): 555–566.

Fink, M. & et. al. (2000). Time-reversed acoustics, *Rep. Progr. Phys* 63: 1988–1955.

Guguen, P. & El Zein, G. (2004). *Les techniques multi-antennes pour les réseaux sans fil*, Hermes Science Publishers.

Khaleghi, A. & El Zein, G. (2007). Signal frequency and bandwidth effects on the performance of UWB time-reversal technique, *Antennas and Propagation Conference, 2007. LAPC 2007, Loughborough*, pp. 97–100.

Khaleghi, A., El Zein, G. & Naqvi, I. (2007). Demonstration of time-reversal in indoor ultra-wideband communication: Time domain measurement, *International Symposium on Wireless Communication Systems, ISWCS 2007*, pp. 465–468.

Kyritsi, P., Eggers, P. & Oprea, A. (2004). MISO time reversal and time compression, *Proc. URSI International Symposium on Electromagnetic Theory*.

Kyritsi, P., Papanicolaou, G., Eggers, P. & Oprea, A. (2004). MISO time reversal and delay-spread compression for FWA channels at 5 ghz, *IEEE Antennas and Wireless Propagation Letters* 3: 96–99.

Lerosey, G., De Rosny, J., Tourin, A., Derode, A. & Fink, M. (2006). Time reversal of wideband microwaves, *Appl. Phys. Lett.* 15: 154101.

Mo, S. S., Guo, N., Zhang, J. Q. & Qiu, R. C. (2007). UWB MISO time reversal with energy detector receiver over ISI channels, *IEEE Consumer Communications and Networking Conference, CCNC2007*, pp. 629–633.

Naqvi, I. & El Zein, G. (2008). Time domain measurements for a time reversal SIMO system in reverberation chamber and in an indoor environment, *Digest of Papers, IEEE International Conference on Ultra-Wideband, ICUWB 2008*, Vol. 2, pp. 211–214.

Naqvi, I. H. & El Zein, G. (2009). Time reversal UWB system: SISO, SIMO, MISO and MIMO comparison with time domain experiments, *Journées Scientifiques CNFRS-URSI "Propagation et Télédétection"*.

Naqvi, I. H. & El Zein, G. (2010). Retournement temporel en ULB: étude comparative par mesures pour des configurations multi-antennes, *Revue de l'Electricité et de l'Electronique (REE). Dossier: Propagation et Télédétection* (2): 66–72.

Naqvi, I., Khaleghi, A. & El Zein, G. (2007). Performance enhancement of multiuser time reversal UWB communication system, *International Symposium on Wireless Communication Systems, ISWCS 2007*, pp. 567–571.

Naqvi, I., Khaleghi, A. & El Zein, G. (2009). Multiuser time reversal uwb communication system: A modified transmission approach, *IEEE International Symposium On Personal, Indoor and Mobile Radio Communications (PIMRC '09)*.

Nguyen, H., Andersen, J. & Pedersen, G. (2005). The potential use of time reversal techniques in multiple element antenna systems, *IEEE Communications Letters* 9(1): 40–42.

Nguyen, H. T., Kovacs, I. & Eggers, P. (2006). A time reversal transmission approach for multiuser UWB communications, *IEEE Transactions on Antennas and Propagation* 54(11): 3216–3224.

Oestges, C., Hansen, J., Emami, S. M., Kim, A. D., Papanicolaou, G. & Paulraj, A. J. (2004). Time reversal techniques for broadband wireless communication systems, *European Microwave Conference (Workshop)*.

Qiu, R., Zhou, C., Guo, N. & Zhang, J. (2006). Time reversal with MISO for ultrawideband communications: Experimental results, *IEEE Antennas and Wireless Propagation Letters* 5(1): 269–273.

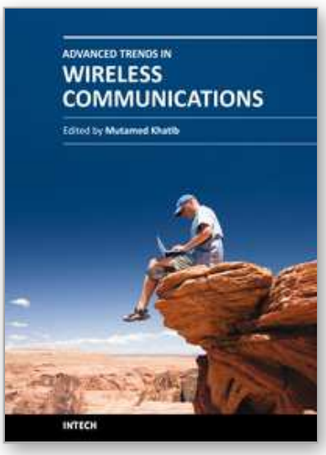

Advanced Trends in Wireless Communications

Edited by Dr. Mutamed Khatib

ISBN 978-953-307-183-1
Hard cover, 520 pages
Publisher InTech
Published online 17, February, 2011
Published in print edition February, 2011

Physical limitations on wireless communication channels impose huge challenges to reliable communication. Bandwidth limitations, propagation loss, noise and interference make the wireless channel a narrow pipe that does not readily accommodate rapid flow of data. Thus, researches aim to design systems that are suitable to operate in such channels, in order to have high performance quality of service. Also, the mobility of the communication systems requires further investigations to reduce the complexity and the power consumption of the receiver. This book aims to provide highlights of the current research in the field of wireless communications. The subjects discussed are very valuable to communication researchers rather than researchers in the wireless related areas. The book chapters cover a wide range of wireless communication topics.

How to reference

In order to correctly reference this scholarly work, feel free to copy and paste the following:

Ijaz Naqvi and Ghaïs El Zein (2011). Time Reversal Technique for Ultra Wide-band and MIMO Communication Systems, Advanced Trends in Wireless Communications, Dr. Mutamed Khatib (Ed.), ISBN: 978-953-307-183-1, InTech, Available from: http://www.intechopen.com/books/advanced-trends-in-wireless-communications/time-reversal-technique-for-ultra-wide-band-and-mimo-communication-systems

INTECH
open science | open minds

InTech Europe
University Campus STeP Ri
Slavka Krautzeka 83/A
51000 Rijeka, Croatia
Phone: +385 (51) 770 447
Fax: +385 (51) 686 166
www.intechopen.com

InTech China
Unit 405, Office Block, Hotel Equatorial Shanghai
No.65, Yan An Road (West), Shanghai, 200040, China
中国上海市延安西路65号上海国际贵都大饭店办公楼405单元
Phone: +86-21-62489820
Fax: +86-21-62489821

IntechOpen